Membrane Reactors

Deutsche Ausgabe: DOI: 10.1002/ange.201602207
Internationale Ausgabe: DOI: 10.1002/anie.201602207

# Integration of Nine Steps into One Membrane Reactor To Produce Synthesis Gases for Ammonia and Liquid Fuel

*Wenping Li, Xuefeng Zhu,* Shuguang Chen, and Weishen Yang**

***Abstract:*** *The synthesis of ammonia and liquid fuel are two important chemical processes in which most of the energy is consumed in the production of $H_2/N_2$ and $H_2/CO$ synthesis gases from natural gas (methane). Here, we report a membrane reactor with a mixed ionic-electronic conducting membrane, in which the nine steps for the production of the two types of synthesis gases are shortened to one step by using water, air, and methane as feeds. In the membrane reactor, there is no direct $CO_2$ emission and no CO or $H_2S$ present in the ammonia synthesis gas. The energy consumption for the production of the two synthesis gases can be reduced by 63 % by using this membrane reactor. This promising membrane reactor process has been successfully demonstrated by experiment.*

Food, energy, and environment are the foundations of human social development. Ammonia, synthesized by the Haber–Bosch process, is the second most produced chemical on the planet,[1] and is used to produce fertilizer to increase food production.[2–4] Natural gas is usually used as a feedstock to produce ammonia synthesis gas (ASG, $H_2/N_2 = 3:1$).[5] This process is accompanied by large atmospheric emissions of $CO_2$ (about $400 \times 10^6$ tons per annum).[6] In a typical ASG production process, six main steps are required to convert cleaned natural gas into ASG: steam reforming, air reforming, water-gas shifting at high and low temperatures, $CO_2$ separation, and methanation (see Figure S1 a in the Supporting Information). This long route for the production of ASG requires huge capital investment and consumes significant amounts of energy. In the entire process for the synthesis of ammonia, ASG production constitutes about 84 % of the energy consumption,[7] while the step corresponding to the catalytic synthesis of ammonia only accounts for a small amount of energy consumption.[8] Gradual improvements in the performance of catalysts for the synthesis of ammonia have resulted in the energy consumption of the catalytic step being reduced close to the theoretical value.[8] Electrochemical approaches have been proposed to directly synthesize ammonia without the production of ASG by using water and nitrogen as the feed gases.[5,9–11] However, the rate of ammonia production, Faraday efficiency, and stability of the electrochemical process still need to be improved significantly. Therefore, the traditional process for the synthesis of ammonia will still prevail in the near future, but great innovation in the ASG production technology is imperative to reduce energy consumption for the industrial synthesis of ammonia.[12]

The Fischer–Tropsch process is an important and feasible route to diversify energy resources.[13–16] Natural gas is a typical feedstock to produce liquid-fuel synthesis gas (LFSG, $H_2/CO = 2:1$) in three main steps: steam reforming, air separation, and mixed reforming. The production of LFSG constitutes the majority of the costs and energy consumption in the entire gas-to-liquid process (see Figure S1 b in the Supporting Information).[17–19] A large portion of energy is consumed by the separation of air to obtain pure oxygen. Partial oxidation of methane (POM) in mixed ionic-electronic conducting (MIEC) membrane reactors, in which air separation and the partial oxidation reaction are coupled, was considered to be a promising route to produce LFSG with a suitable $H_2/CO$ ratio (2:1) and high energy efficiency.[19–21] However, process safety is still a great challenge if the ceramic MIEC membranes break during the on-stream operation. Additionally, the temperature runaway induced by the fast exothermal reaction is difficult to avoid in a large-scale MIEC membrane reactor. Therefore, process risks need to be eliminated before commercialization of the MIEC membrane syngas technology.

In recent years, coupling catalytic reactions in membrane reactors has been regarded as an efficient way to achieve process intensification.[22,23] Ammonia synthesis, conversion of benzene into phenol, and water splitting have been performed with high efficiency in membrane reactors.[24–31] Here, we present a membrane reactor with an MIEC membrane and catalyst to coproduce ASG and LFSG from water, air, and methane in one step (see Figure S1 c in the Supporting Information). Figure 1 a shows the concept of the membrane reactor. Air and water with an appropriate ratio are fed to one side (side I) of the membrane, while methane is fed to the other side (side II). At high temperatures, oxygen molecules from the air on side I permeate as oxygen ions through the MIEC membrane by diffusion to side II, where they react with methane to form LFSG, meanwhile electrons

[*] W. P. Li, Prof. X. F. Zhu, Prof. W. S. Yang
State Key Laboratory of Catalysis
Dalian Institute of Chemical Physics
Chinese Academy of Sciences
457 Zhongshan Road, Dalian 116023 (China)
E-mail: zhuxf@dicp.ac.cn
yangws@dicp.ac.cn
Prof. S. G. Chen
Dalian National Laboratory for Clean Energy
Dalian Institute of Chemical Physics
Chinese Academy of Sciences
457 Zhongshan Road, Dalian 116023 (China)
W. P. Li
University of Chinese Academy of Sciences
Beijing, 100049 (China)
Supporting information and the ORCID identification number(s) for the author(s) of this article can be found under http://dx.doi.org/10.1002/anie.201602207.

 © 2016 Wiley-VCH Verlag GmbH & Co. KGaA, Weinheim 

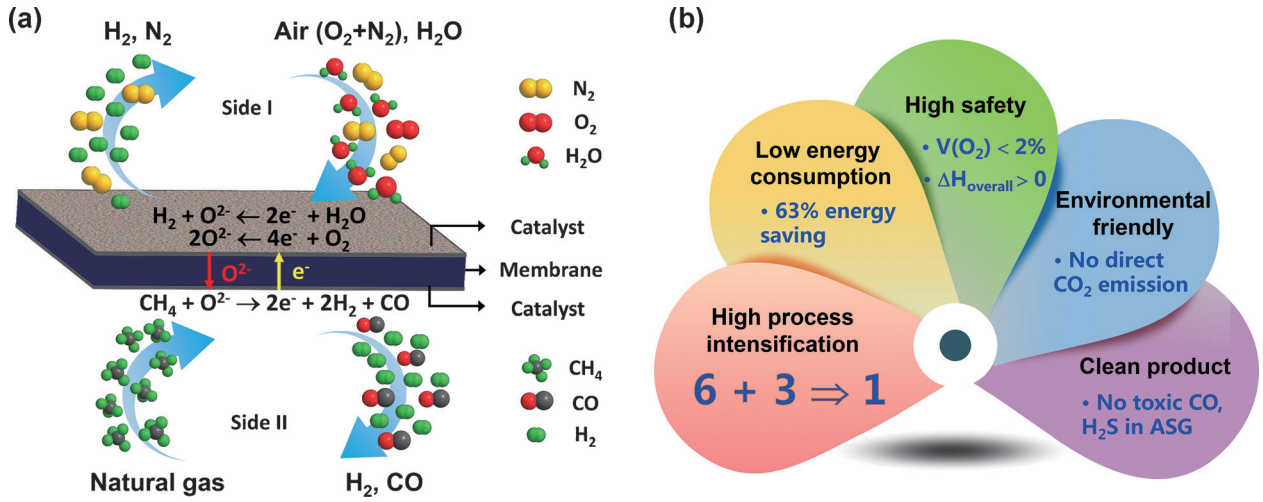


***Figure 1.*** a) Concept of the one-step production of the two synthesis gases for ammonia ($H_2/N_2 = 3:1$) and liquid fuel ($H_2/CO = 2:1$) from water, air, and natural gas in a membrane reactor. b) Merits of the membrane reactor for the production of ASG and LFSG compared with industrial processes. "6" represents a six-step process for the industrial production of ASG; "3" represents a three-step process for the industrial production of LFSG; "1" represents the one-step process for the coproduction of ASG and LFSG in the membrane reactor.

migrate from side II to side I to maintain the electric neutrality of the whole process. The LFSG has an extremely low oxygen partial pressure (for example, $10^{-21}$ atm) on side II, which drives the permeation of oxygen from side I to side II. In this process, the amount of oxygen in the air is limited in the feed, thus oxygen molecules can completely permeate to side II. When the oxygen partial pressure of side I decreases to a value that allows water splitting, hydrogen is produced. Thermodynamic calculations (see Figure S2 in the Supporting Information) show that the equilibrium conversion of the water-splitting reaction can be as high as 96% at 900 °C if oxygen can be removed rapidly by the POM reaction through the MIEC membrane. Under steady operating conditions, oxygen from the air and water splitting continuously permeates through the MIEC membrane and reacts with methane. Therefore, the resultant gases on side I with a suitable $H_2/N_2$ ratio are ready for the synthesis of ammonia after drying; simultaneously, the produced LFSG on side II with a suitable $H_2/CO$ ratio is ready for the synthesis of liquid fuel.

The merits of the membrane reactor are summarized in Figure 1b. The most important advantage of the membrane reactor is to shorten the six-step process (steam reforming, air reforming, water-gas shifting at high and low temperatures, $CO_2$ separation, and methanation) for ASG production and the three-step process (steam reforming, air separation, and mixed reforming) for LFSG production to a one-step process. The highly integrated membrane reactor allows much higher energy efficiency (ca. 63% energy saving) than the traditional complex processes. An air separation unit is also integrated into the membrane reactor during the production of LFSG. Besides the strong integration and high energy efficiency, the additional merits of this membrane reactor include high safety, environmental friendliness, and clean product (Figure 1b). Unlike traditional MIEC membrane reactors for POM to syngas, no safety problem exists even if the ceramic MIEC membranes break during the operation, since the volume fraction of oxygen in the feed (including air, steam, and methane) is too low (<2%) for explosions. Temperature runaway in POM cannot happen in this new conceptual membrane reactor, since the exothermic reaction is coupled with a strong endothermic water splitting reaction. The process in the MIEC membrane reactor can be described according to Equation (1):

$$\frac{1}{7}\left(6\,H_2O + 2\,N_2 + \frac{1}{2}O_2\right)_{\text{side I}} + (CH_4)_{\text{side II}} \xrightarrow{MR} \xrightarrow{MR} \frac{2}{7}(3\,H_2 + N_2)_{\text{side I}} + (2\,H_2 + CO)_{\text{side II}} \quad (1)$$

$$\Delta H_{900\,^\circ C} = 190\ \text{kJ mol}^{-1}$$

$$\Delta G_{900\,^\circ C} = -103\ \text{kJ mol}^{-1}.$$

In the membrane reactor, ASG is produced without $CO_2$ emissions, and no CO or $H_2S$ are present (both are strong poisons of the catalyst for the synthesis of ammonia). Thus, $CO_2$ separation and methanation are unnecessary.

The rates of production for ASG and LFSG depend on the oxygen permeation flux of the MIEC membranes, which can be described by the Wagner equation [Eq. (2)] if the electronic and ionic conductivities ($\sigma_e$ and $\sigma_i$) of the membrane materials are constant under the range of oxygen partial pressures of the catalytic membrane reactions [Eq. (2)]:

$$J_{O_2} = -\frac{RT}{16F^2L}\frac{\sigma_e + \sigma_i}{\sigma_e \sigma_i}\ln\frac{P'_{O_2}}{P''_{O_2}} \quad (2)$$

Here, $R$, $T$, $F$, and $L$ are the gas constant, temperature, Faraday constant, and membrane thickness, respectively.[32] For a certain MIEC membrane, oxygen permeation occurs as long as the oxygen partial pressure of side I is higher than that of side II. To realize this attractive concept, the selected MIEC membrane should be stable in a strong reducing atmosphere and exhibit high oxygen permeability. Furthermore, the catalysts used in the membrane reactor should

 © 2016 Wiley-VCH Verlag GmbH & Co. KGaA, Weinheim 

exhibit high catalytic activity and stability for the water splitting and POM reactions, respectively.

A perovskite-type MIEC $Ba_{0.98}Ce_{0.05}Fe_{0.95}O_{3-\delta}$ (BCF) membrane was chosen as an example to demonstrate and confirm the concept after we considered the balance between stability and permeability. The oxygen permeation flux of BCF is 1.3 $mL\,cm^{-2}\,min^{-1}$ under an air/He gradient, and it is even stable in a $H_2$ atmosphere at 900 °C (see Figure S3 and S4 in the Supporting Information). The membranes were sealed in the membrane reactor by silver paste between two alumina tubes to separate the oxygen of side I from side II (see Figure S5 in the Supporting Information). Here, a Ru-based catalyst prepared by impregnating $RuCl_3$ into $Ce_{0.85}Sm_{0.15}O_{2-\delta}$ (1 wt% Ru/SDC) was used to catalyze the POM reaction for the production of LFSG. This catalyst has a particle size of about 100 nm and a specific surface area of 19 $m^2\,g^{-1}$. Fortunately, we found that the 1 wt% Ru/SDC catalyst, which is designed for the production of LFSG, also exhibits a high catalytic activity and stability for the production of ASG.

In previous studies on MIEC membrane reactors, dilute $CH_4$ was used to avoid coke deposition and temperature runaway.[20,33] Here, the effects of $CH_4$ concentration on $CH_4$ conversion, CO selectivity on side II, and ASG production rate on side I were tested at a given $CH_4$ flow rate of 7.0 $mL\,min^{-1}$ on side II and a fixed $H_2/N_2$ ratio of 3:1 on side I to find the optimal $CH_4$ concentration at 900 °C (see Figure S6 in the Supporting Information). The $CH_4$ conversion and CO selectivity increase gradually as the concentration of $CH_4$ increases, whereas the ASG production rate stays almost constant at 13.5 $mL\,cm^{-2}\,min^{-1}$. In a practical operation, a pure $CH_4$ feed is better than dilute $CH_4$ since no additional separation step is required to remove the diluting gas. Thus, in the following experiments, pure methane was used as the feed to side II. Figure 2 shows the effects of the $CH_4$ flow rate on its conversion, CO selectivity, as well as LFSG and ASG production rates at 900 °C. The $H_2/N_2$ ratio was fixed at 3:1 by adjusting the flow rates of air. As the $CH_4$ flow rate increases from 3.0 to 10.0 $mL\,min^{-1}$, the ASG and LFSG production rates increase from 9.1 to 13.5 $mL\,cm^{-2}\,min^{-1}$ on side I and from 8.6 to 36.7 $mL\,cm^{-2}\,min^{-1}$ on side II. At the same time, the CO selectivity increases gradually from 70.4 to 99.3% and the $CH_4$ conversion decreases gradually from 97.8 to 88.1%. Simultaneously, a suitable $H_2/CO$ ratio of 2:1 was achieved because of the highly selective POM reaction. The experiments successfully demonstrate that the membrane reactor shown in Figure 1a can simultaneously produce ASG with a high production rate and a suitable $H_2/N_2$ ratio on side I as well as LFSG with a high production rate and suitable $H_2/CO$ ratio on side II.

In the membrane reactor, three processes are coupled together: water splitting, oxygen permeation across the MIEC membrane, and POM. All the processes can be accelerated by increasing the temperature. Thus, to maintain CO selectivity greater than 95% and to achieve a maximum $CH_4$ conversion at each temperature, the optimal feed rate of $CH_4$ needed to be adjusted as the temperature was varied (see Figure S7 in the Supporting Information). In general, the optimal feed rate of $CH_4$ increases with temperature. The effects of temperature on $CH_4$ conversion, CO selectivity, and ASG and LFSG production rates were thus investigated (Figure 3a). It was found that the $CH_4$ conversion increases gradually with temperature, and a high $CH_4$ conversion (> 95%) can be achieved above 875 °C. The ASG and LFSG production rates increase from 4.3 to 18.8 $mL\,cm^{-2}\,min^{-1}$ on side I and from

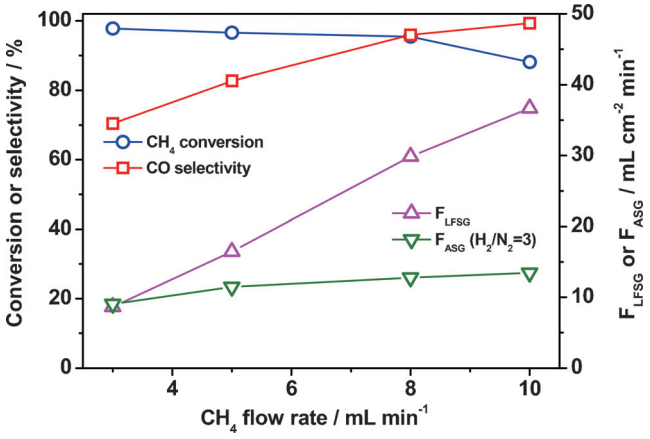


*Figure 2.* Effects of $CH_4$ flow rate on $CH_4$ conversion, CO selectivity, as well as ASG and LFSG production rates at 900 °C. $H_2O$ steam: 200 $mL\,min^{-1}$.

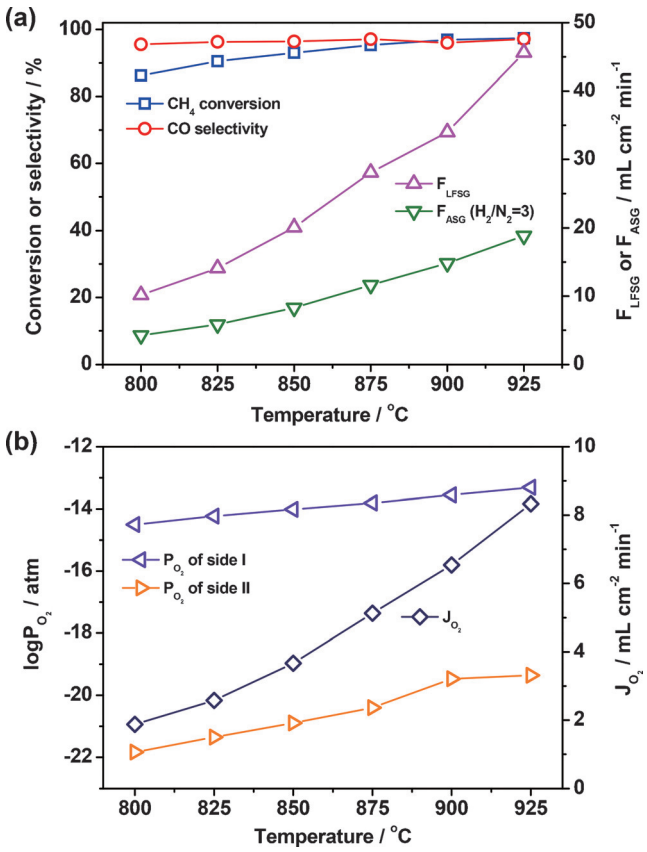


*Figure 3.* Effects of temperature on performance. a) $CH_4$ conversion, CO selectivity, as well as ASG and LFSG production rates. b) Oxygen permeation flux and the oxygen partial pressures for the two sides of the membrane. $H_2/N_2 = 3:1$ on side I of the membrane, $H_2O$ steam: 200 $mL\,min^{-1}$.


© 2016 Wiley-VCH Verlag GmbH & Co. KGaA, Weinheim

10.2 to 45.6 mL cm$^{-2}$ min$^{-1}$ on side II, respectively, as the temperature increases from 800 to 925 °C. Although both sides have $H_2$-containing atmospheres, a large oxygen partial pressure gradient ($10^6$–$10^7$) exists across the membrane (Figure 3b). It is the oxygen partial pressure gradient that drives oxygen on side I to permeate through the membrane to side II. The corresponding oxygen permeation flux through the membrane increases from 1.9 to 8.3 mL cm$^{-2}$ min$^{-1}$ as the temperature increases from 800 to 925 °C. There was no residual oxygen detected on side I, because the concentration of hydrogen produced from water splitting on side I reached 1.1–5.0 vol% in the temperature range 800–925 °C and the corresponding oxygen partial pressures were in the range of $10^{-13}$–$10^{-15}$ atm. After temperature-dependent experiments over 110 h, the membrane reactor was subjected to constant operation conditions (Figure 4). A stable membrane reactor

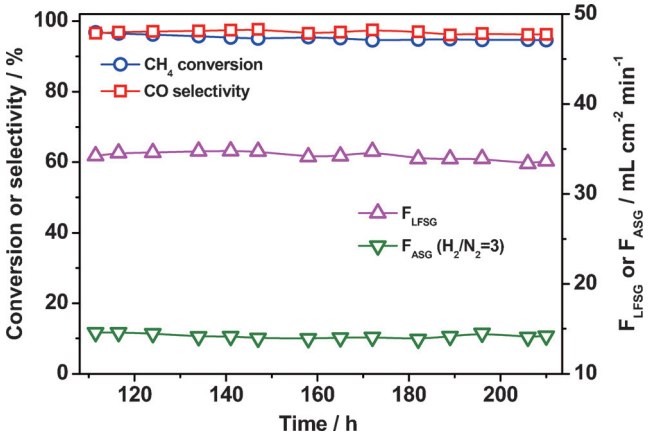


***Figure 4.*** Stable operation of the membrane reactor for the production of ASG and LFSG at 900 °C. $H_2O$ steam: 200 mL min$^{-1}$; $CH_4$: 9.0 mL min$^{-1}$.

operation was observed over 100 h of on-stream processing. The carbon balance stayed in the range of 95–99%. $CH_4$ conversion and CO selectivity were high (94–98%), and the ASG ($H_2/N_2 = 3:1$) and LFSG ($H_2/CO = 2:1$) production rates remained at about 14 and 34 mL cm$^{-2}$ min$^{-1}$, respectively. These results indicate that the membrane reactor can be steadily operated to coproduce ASG and LFSG in a highly efficient manner. After operation for a total of 210 h, both sides of the membrane close to the surfaces remain very similar to the as-prepared membrane (see Figure S8a in the Supporting Information), as evident by comparing the cross-sectional views (see Figure S8b,c in the Supporting Information). Energy dispersive spectroscopy (EDS) analysis show there is no apparent change in the elemental composition of the bulk area of the membrane (see Table S1 in the Supporting Information). Thermodynamic calculations show that no $BaCO_3$ forms during the 100 h on-stream experiment at 900 °C, where the $CO_2$ partial pressure was in the range of 0.8 to 1.3 kPa (see Figure S9 in the Supporting Information). The catalyst layers coated on both sides exfoliated partially from the membrane surfaces after the membrane reactor cooled to room temperature. A thermogravimetric/differential thermal analysis (TG-DTA) experiment on the spent catalyst showed that no carbon deposition had occurred (see Figure S10 in the Supporting Information). Beneath the catalyst layers, the chemical composition of the membrane surface is similar to that of the fresh surface (see Table S1 in the Supporting Information). This finding indicates that the membrane material is stable under such reaction conditions.

To save energy in steam heating on side I, it is economic to reduce the flow rate of the water steam in a practical operation. Figure 5 shows the effects of $H_2O/CH_4$ molar ratio

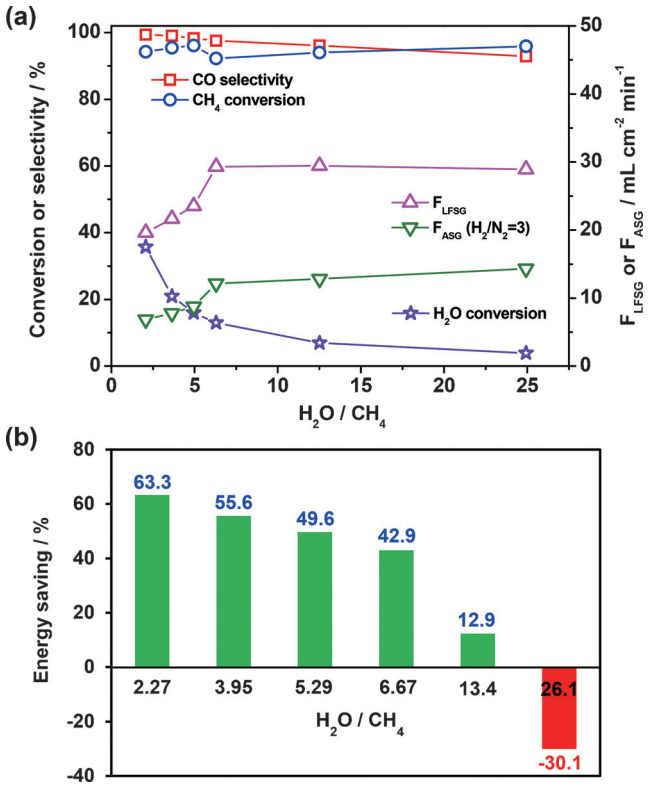


***Figure 5.*** Effects of $H_2O/CH_4$ molar ratios on performance. a) $H_2O$ conversion and ASG and LFSG production rates at a $H_2/N_2$ ratio of 3:1 at 900 °C. b) Energy saving in the membrane reactor. The values of the energy savings were calculated from energy consumptions in the membrane reactor and industrial energy consumption when producing the same amount of ASG and LFSG.

on $CH_4$ conversion, CO selectivity, $H_2O$ conversion, as well as ASG and LFSG production rates at a $H_2/N_2$ ratio of 3:1 and 900 °C. At all the reaction conditions tested, the $CH_4$ conversion and CO selectivity remained in the range of 92.0 to 99.5%. The $H_2/N_2$ ratio can be adjusted over a wide range by changing the air flow rate, which allows the membrane reactor to produce $H_2/N_2$ synthesis gas in various ratios (see Figure S11 in the Supporting Information). The ASG and LFSG production rates increase with the $H_2O/CH_4$ ratio, whereas the $H_2O$ conversion decreases (Figure 5a and see Figure S12 in the Supporting Information). As the $H_2O/CH_4$ molar ratio was decreased to 2.07:1, the water conversion reached a high value of 35.75%, which is approximately $8 \times 10^4$ times higher than the equilibrium conversion (0.00046%) of the water splitting reaction at 900 °C. The $H_2O/CH_4$ molar

 © 2016 Wiley-VCH Verlag GmbH & Co. KGaA, Weinheim 

ratio is lower than that used in the industrial processes for the production ASG and LFSG, in which a ratio of about 3.5:1 is usually used. The energy consumption in the membrane reactor for the production of ASG and LFSG on an industrial scale was calculated by using SIMSCI-PRO II 5.5 and ChemCAD 6.1.2 (see Figure S13 and Table S2 in the Supporting Information). A 63.3% saving in energy consumption compared with traditional industrial processes can be achieved at a $H_2O/CH_4$ molar ratio of 2.27:1, and the membrane reactor process achieves an energy saving as long as the $H_2O/CH_4$ molar ratio is lower than about 14:1 (Figure 5b and see Table S3 in the Supporting Information). The membrane reactor allows a highly integrated process that can shorten the nine steps for the generation of ASG and LFSG to one step, and thus decrease the energy consumption significantly.

In summary, we have demonstrated a new concept of a membrane reactor for the highly efficient production of ASG and LFSG. The success with this new concept may trigger innovation in traditional natural gas chemical industries.

## Acknowledgements

We thank the National Natural Science Foundation of China (21476225, U1508203 and 91545202), the Strategic Priority Research Program of the Chinese Academy of Sciences (Grant XDB17020400), Youth Innovation Promotion Association of the Chinese Academy of Sciences, and DICP (DICP DMTO201503) for financial support.

**Keywords:** membranes · process intensification · synthesis gas · synthetic methods · water splitting

**How to cite:** *Angew. Chem. Int. Ed.* **2016**, *55*, 8566–8570
*Angew. Chem.* **2016**, *128*, 8708–8712

[1] R. Mendivil, U. Fischer, M. Hirao, K. Hungerbühler, *Int. J. Life Cycle Assess.* **2006**, *11*, 98–105.
[2] J. W. Erisman, M. A. Sutton, J. Galloway, Z. Klimont, W. Winiwarter, *Nat. Geosci.* **2008**, *1*, 636–639.
[3] J. N. Galloway, A. R. Townsend, J. W. Erisman, M. Bekunda, Z. C. Cai, J. R. Freney, L. A. Martinelli, S. P. Seitzinger, M. A. Sutton, *Science* **2008**, *320*, 889–892.
[4] T. Kandemir, M. E. Schuster, A. Senyshyn, M. Behrens, R. Schlögl, *Angew. Chem. Int. Ed.* **2013**, *52*, 12723–12726; *Angew. Chem.* **2013**, *125*, 12955–12959.
[5] S. Licht, B. C. Cui, B. H. Wang, F. F. Li, J. Lau, S. Z. Liu, *Science* **2014**, *345*, 637–640.
[6] H. Z. Liu, *Chin. J. Catal.* **2014**, *35*, 1619–1640.
[7] R. Michalsky, B. J. Parman, V. Amanor-Boadu, P. H. Pfromm, *Energy* **2012**, *42*, 251–260.
[8] N. Saadatjou, A. Jafari, S. Sahebdelfar, *Chem. Eng. Commun.* **2015**, *202*, 420–448.
[9] I. A. Amar, R. Lan, C. T. G. Petit, S. W. Tao, *J. Solid State Electrochem.* **2011**, *15*, 1845–1860.
[10] S. Giddey, S. P. S. Badwal, A. Kulkarni, *Int. J. Hydrogen Energy* **2013**, *38*, 14576–14594.
[11] A. Skodra, M. Stoukides, *Solid State Ionics* **2009**, *180*, 1332–1336.
[12] R. Schlögl, *Angew. Chem. Int. Ed.* **2003**, *42*, 2004–2008; *Angew. Chem.* **2003**, *115*, 2050–2055.
[13] T. Takeshita, K. Yamaji, *Energy Policy* **2008**, *36*, 2773–2784.
[14] A. J. Ragauskas, C. K. Williams, B. H. Davison, G. Britovsek, J. Cairney, C. A. Eckert, W. J. Frederick, Jr., J. P. Hallett, D. J. Leak, C. L. Liotta, J. R. Mielenz, R. Murphy, R. Templer, T. Tschaplinski, *Science* **2006**, *311*, 484–489.
[15] V. R. Calderone, N. R. Shiju, D. Curulla-Ferré, S. Chambrey, A. Khodakov, A. Rose, J. Thiessen, A. Jess, G. Rothenberg, *Angew. Chem. Int. Ed.* **2013**, *52*, 4397–4401; *Angew. Chem.* **2013**, *125*, 4493–4497.
[16] C. X. Xiao, Z. P. Cai, T. Wang, Y. Kou, N. Yan, *Angew. Chem. Int. Ed.* **2008**, *47*, 746–749; *Angew. Chem.* **2008**, *120*, 758–761.
[17] D. J. Wilhelm, D. R. Simbeck, A. D. Karp, R. L. Dickenson, *Fuel Process. Technol.* **2001**, *71*, 139–148.
[18] K. Aasberg-Petersen, C. S. Nielsen, I. Dybkjær, J. Perregaard, "Large Scale Methanol Production from Natural Gas", can be found under http://topsoe.ru/sites/default/files/topsoe_large_scale_methanol_prod_paper.ashx_.pdf, **2008**.
[19] U. Balachandran, J. T. Dusek, R. L. mieville, R. B. Poeppel, M. S. Kleefisch, S. pei, T. P. kobylinski, C. A. Udovich, A. C. Bose, *Appl. Catal. A* **1995**, *133*, 19–29.
[20] J. H. Tong, W. S. Yang, R. Cai, B. C. Zhu, L. W. Lin, *Catal. Lett.* **2002**, *78*, 129–137.
[21] X. F. Zhu, Q. M. Li, Y. F. He, Y. Cong, W. S. Yang, *J. Membr. Sci.* **2010**, *360*, 454–460.
[22] M. P. Dudukovic, *Science* **2009**, *325*, 698–701.
[23] S. A. Bhat, J. Sadhukhan, *AIChE J.* **2009**, *55*, 408–422.
[24] Z. W. Cao, H. Q. Jiang, H. X. Luo, S. Baumann, W. A. Meulenberg, J. Assmann, L. Mleczko, Y. Liu, J. Caro, *Angew. Chem. Int. Ed.* **2013**, *52*, 13794–13797; *Angew. Chem.* **2013**, *125*, 14039–14042.
[25] J. Pérez-Ramírez, B. Vigeland, *Angew. Chem. Int. Ed.* **2005**, *44*, 1112–1115; *Angew. Chem.* **2005**, *117*, 1136–1139.
[26] R. Lan, J. T. S. Irvine, S. W. Tao, *Sci. Rep.* **2013**, *3*, 1145.
[27] S. Niwa, M. Eswaramoorthy, J. Nair, A. Raj, N. Itoh, H. Shoji, T. Namba, F. Mizukami, *Science* **2002**, *295*, 105–107.
[28] H. Q. Jiang, H. H. Wang, S. Werth, T. Schiestel, J. Caro, *Angew. Chem. Int. Ed.* **2008**, *47*, 9341–9344; *Angew. Chem.* **2008**, *120*, 9481–9484.
[29] C. Y. Park, T. H. Lee, S. E. Dorris, U. Balachandran, *ECS Trans.* **2008**, *13*, 393–403.
[30] H. Q. Jiang, Z. W. Cao, S. Schirrmeister, T. Schiestel, J. Caro, *Angew. Chem. Int. Ed.* **2010**, *49*, 5656–5660; *Angew. Chem.* **2010**, *122*, 5790–5794.
[31] A. Thursfield, A. Murugan, R. Franca, I. S. Metcalfe, *Energy Environ. Sci.* **2012**, *5*, 7421–7459.
[32] J. Sunarso, S. Baumann, J. M. Serra, W. A. Meulenberg, S. Liu, Y. S. Lin, J. C. Diniz da Costa, *J. Membr. Sci.* **2008**, *320*, 13–41.
[33] H. H. Wang, C. Tablet, T. Schiestel, S. Werth, J. Caro, *Catal. Commun.* **2006**, *7*, 907–912.

Received: March 3, 2016
Published online: June 6, 2016

 © 2016 Wiley-VCH Verlag GmbH & Co. KGaA, Weinheim 